ICE-PoGO: Improving Dynamic Panoramic Reconstruction of 4D ICE Imaging through Pose Graph Optimization

Sebastian Herz[1,2], Magdalena Wysocki[2,3], Felix Tristram[2,3], Julia Hickler[1], Lydia Neary-Zajiczek[1], Christoph Hennersperger[1], Nassir Navab[2,3], and Stefan Wörz[1]

[1] LUMA Vision, Beech Hill Road, Dublin, Ireland
http://www.lumavision.com
{sebastian.herz, julia.hickler, lydia.neary-zajiczek, christoph.hennersperger, stefan.woerz}@lumavision.com
[2] Chair for Computer Aided Medical Procedures (CAMP), Technical University of Munich, Germany
{magdalena.wysocki, felix.tristram, nassir.navab}@tum.de
[3] Munich Center for Machine Learning (MCML), Munich, Germany

Abstract. Intracardiac echocardiography (ICE) has the potential to play a crucial role in structural heart disease (SHD) interventions by providing high-quality imaging in real time, without many of the key drawbacks of established imaging modalities. However, ICE's limited field-of-view (FoV) requires continuous readjustments of the catheter position to fully visualize the dynamic cardiac environment, which impairs spatial navigation and increases procedure time and complexity. Dynamic panoramic reconstruction can mitigate this limitation. However, state-of-the-art methods depend on precise catheter tracking, the accuracy of which is affected by the presence of noise and anatomical motion. While registration can correct these errors, existing approaches are computationally prohibitive for large imaging volumes due to repeated iterations over image data, further amplified by the added time dimension. To address these challenges, we present a novel method for truly dynamic panoramic reconstruction by leveraging the repetitive nature of cardiac motion under a cyclic environment assumption. To our knowledge, our method is the first to employ dynamic pose graph optimization (PGO) specifically designed for 4D ICE tracking. Our results demonstrate enhanced tracking accuracy and improved panoramic reconstruction quality, potentially providing real-time, dynamic anatomical guidance for clinicians. The improved alignment of overlapping ICE volumes and increased temporal tracking resolution represent a substantial advancement in 4D ICE imaging, enhancing navigation and decision-making during complex cardiac interventions.

Keywords: dynamic panoramic reconstruction · intracardiac echocardiography · pose graph optimization.

1 Introduction

Intracardiac echocardiography (ICE) is an ultrasound (US) modality that assists or replaces transesophageal echocardiography (TEE) in structural heart disease procedures [1, 6, 14, 16], reducing the risks associated with general anesthesia and providing an alternative for patients at high risk of complications due to esophageal or gastric disease, where the use of TEE remains limited [13, 3]. However, ICE's limited field of view (FoV) makes navigation within the heart difficult, often requiring fluoroscopy for guidance, which introduces radiation exposure. Reconstruction of a larger FoV from multiple overlapping ICE volumes and its visualization assists physicians in navigating the ICE catheter and tools during procedures. Still, an accurate reconstruction is difficult to achieve due to the highly dynamic environment and noise affecting the accuracy of electromagnetic tracking of the imaging catheter's position.

Dynamic panoramic reconstruction in ICE addresses the problem of generating a wide FoV image that captures cardiac anatomy at multiple phases from different views and time points. Existing methods for static panoramic reconstruction [11, 17, 18], neglect the dynamic aspects of the environment, and assume a change in image content arises only from a change in the pose of the imaging device. In the case of cardiac imaging, the heartbeat deforms anatomical structures, violating this assumption and rendering these methods unsuitable for dynamic cases or multiple cardiac phases. In the line of static methods, an ICE-specific static panoramic reconstruction was proposed in [5], fusing electrocardiogram (ECG) gated US volumes based on electromagnetic (EM) tracking supported by sequential registration. Sequential registration can suffer from drift, and EM tracking is noise-prone [2], so acquiring an anatomically aligned panoramic reconstruction is not always possible. Simultaneous localization and mapping (SLAM) methods have been explored for ICE imaging, such as the GridSLAM approach by Koolwal et al. [8] for reconstructing an ECG-gated left atrium. However, extending this to a 4D (3D + t) map would require maintaining multiple explicit 4D map hypotheses, making the approach computationally too expensive. While ECG gating enables static panoramic reconstruction, it restricts an image-based catheter pose update rate to 1–2 Hz, making navigation cumbersome. Mao [10] introduced a dynamic direct simultaneous registration (D-DSR) method for 3D TEE, enabling dynamic reconstruction across multiple phases. However, its scalability is limited, with runtimes increasing significantly as the number of volumes grows[4]. Given ICE's narrower FoV, lower signal-to-noise ratio at image borders due to unfocused transmission, and the need for volumes of multiple phases, reconstructions may involve up to 100 volumes, making D-DSR impractical for clinical applications.

Other possible optimization methods, such as pose graph optimization (PGO), do not have an explicit representation of the reconstructed volume, and their measurements (pairwise registration) scale linearly in runtime with the number

[4] For six volumes, an iteration takes 78 seconds, requiring 10–50 iterations to converge. For eight volumes, iteration time increases to 124 seconds with the same voxel count.

of US volumes. PGO is used in SLAM and reconstruction to refine estimated poses by minimizing the error between measurements, ensuring global consistency in a set of transformations. PGO in intravascular US imaging has been proposed for registering pullbacks taken at different times [19], however, without considerations of a dynamic environment.

To address the issues of a static environment assumption and the prohibitive computational requirements of [5, 8, 10], we propose a method to improve the dynamic panoramic reconstruction of 4D ICE imaging by utilizing PGO. We extend a static environment assumption to a cyclic environment assumption, allowing us to model the repetitive deformation of the cardiac cycle. The cyclic environment assumption allows the environment to change predictably over a finite time, returning to its initial state. From this assumption, the cardiac anatomy appears static when observed at the same point of the cardiac cycle over time. This allows us to build a hypergraph, a graph of pose graphs per discrete time step in the cardiac cycle. A single pose graph per cardiac cycle optimizes the ICE catheter pose by combining a registration scheme with EM tracking (which provides direct 3D pose measurements), ensuring an accurate and globally aligned reconstruction. At the same time, the hypergraph ensures a spatially consistent dynamic panoramic reconstruction across cardiac phases. To support a larger number of US volumes while ensuring computational efficiency suitable for clinical applications, we restrict image information usage to pairwise registration, thereby reducing the parameter search space in computationally expensive optimization. In contrast, global pose refinement, which involves a larger parameter space, is efficiently handled by PGO in SE(3), the special Euclidean group representing 3D rotations and translations. To summarize our contributions:

- Development of the first method for dynamic panoramic reconstruction tailored specifically to ICE imaging, enabling higher temporal resolution in catheter navigation.
- Introduction of PGO approach for dynamic panoramic reconstruction, enabling efficient optimization of poses of large number of US volumes suitable for 4D ICE imaging.
- Demonstration of a major improvement in dynamic panoramic reconstruction in ICE imaging enabled by the improved tracking of the 4D ICE catheter.

2 Method

2.1 Fundamentals

The PGO graph consists of nodes, which are connected through edges. $\mathbf{x} = (\mathbf{x}_1, ..., \mathbf{x}_T)^\top$ is a vector, where $\mathbf{x}_i$ is the pose of node i. $\mathbf{z}_{ij}$ and $\mathbf{\Omega}_{ij}$ represent a measurement as an edge and are the mean and the information matrix of a geometric transform between node i and node j, respectively, where the information matrix holds the uncertainties. $\hat{\mathbf{z}}_{ij}(x_i, x_j)$ is the expected measurement.

Let $\mathbf{F}(\mathbf{x})$ be the negative log-likelihood of all measurements

$$\mathbf{F}(\mathbf{x}) = \sum_{\langle i,j \rangle \in \mathcal{C}} \mathbf{e}_{ij} \left(\mathbf{x}_i, \mathbf{x}_j\right)^T \mathbf{\Omega}_{ij} \mathbf{e}_{ij} \left(\mathbf{x}_i, \mathbf{x}_j\right) \tag{1}$$

where $\mathbf{e}_{ij} \left(\mathbf{x}_i, \mathbf{x}_j\right) = \mathbf{z}_{ij} - \hat{\mathbf{z}}_{ij} \left(\mathbf{x}_i, \mathbf{x}_j\right)$ is the difference between the expected and real measurement, and $\mathcal{C}$ is the set of all pairs. We seek the configuration of nodes $\mathbf{x}^*$ that minimizes the negative log-likelihood $\mathbf{F}(\mathbf{x})$ [4].

2.2 Dynamic Reconstruction

To account for dynamic environments, a 4D pose graph is proposed that optimizes the trajectory of the tip of the ICE catheter over multiple cardiac phases simultaneously. Based on the cyclic environment assumption, the heart rhythm is discretized in the c_n phases. As the heart is assumed static within each cardiac phase c_n, a pose graph is constructed per phase, referred to as an intra-phase graph (see Sect. 2.3). Cardiac phase assignment is commonly performed using ECG gating [8, 11], which ensures robustness to heart rate variability and allows exclusion of anomalous images in the presence of irregular rhythms, as often encountered in structural heart procedures. Each newly acquired US volume can be assigned to one of the intra-phase graphs. To regularize drift between intra-phase graphs, inter-phase edges (see Sec. 2.4) are introduced. This allows us to jointly optimize all poses for all cardiac phases through a single hyper pose graph. Fig. 1 visualizes the concept of building a hyper pose graph out of multiple pose graphs per cardiac phase and connecting them via inter-phase edges.

Given a sequence of US acquisitions, we have a series of states where the state vector of a US volume can be expressed as $\mathbf{x}_t = [\mathbf{p}_t, \mathbf{q}_t, \mathbf{\Theta}_t, c_n]^T$ where $\mathbf{p}_t \in \mathbf{R}^3$ is the 3D position, $\mathbf{q}_t \in \mathbf{R}^4$ is the 3D orientation as a quaternion and $\mathbf{\Theta}_t$ is the acquired US volume at time t, where c_n is a scalar value that represents a phase in the cardiac cycle. The dynamic panoramic reconstruction $\mathbf{m}_{4D}$ is a collection of 4D fused volumes, and is denoted by

$$\mathbf{m}_{4D} = \{v_{i,j,k}(c) \mid v_{i,j,k}(c) \in \mathbf{N},\ c \in \{c_0, c_1, ..., c_n\}\}, \tag{2}$$

where $v_{i,j,k}(c)$ represents the brightness value of the voxel at grid coordinates (i, j, k) that belongs to a discretized cardiac phase c_n. $v_{i,j,k}(c)$ is defined as

$$v_{i,j,k}(c) = f(\mathbf{T}_{\mathbf{p}_t,\mathbf{q}_t}(\mathbf{\Theta}_t(c))) \tag{3}$$

where $\mathbf{T}_{\mathbf{p}_t,\mathbf{q}_t}$ is a homogeneous transform that maps voxel intensities $\mathbf{\Theta}_t(c)$ of discrete cardiac phase c_n into the reconstruction and f is a function that fuses voxels into the reconstruction grid. To replay the reconstruction $\mathbf{m}_{4D}$, $v_{i,j,k}(c)$ is displayed iterating over c according to the patients heart rate.

2.3 Intra-Phase Graph

The intra-phase graph defines the nodes and edges of a single cardiac phase, where the environment is assumed to be static. $\mathbf{x}_i$ represents the position $\mathbf{p}_t$ and

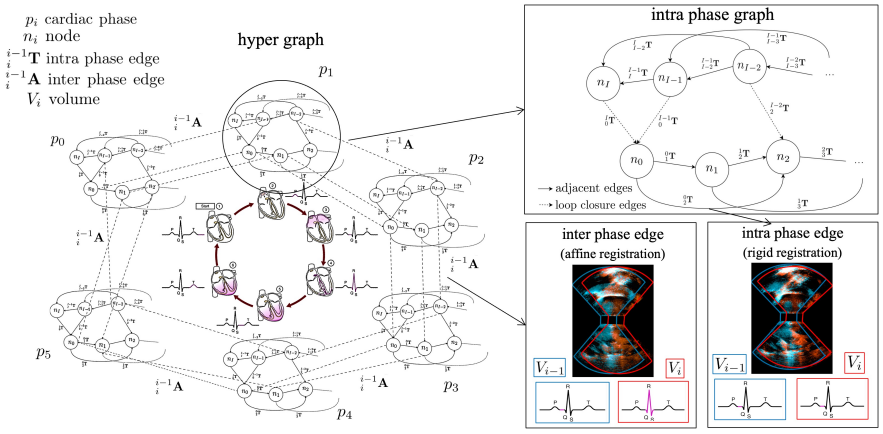

Fig. 1. Concept of a hyper pose graph which connects intra-phase graphs per cardiac phase through inter-phase edges. An intra-phase graph is shown at an enlarged scale. Image adapted from [12], used under CC BY 4.0.

orientation $\mathbf{q}_t$ of a US volume $\mathbf{\Theta}_i$. Given two poses $\mathbf{x}_i$ and $\mathbf{x}_j$ with overlapping observed data $\mathbf{\Theta}_i$ and $\mathbf{\Theta}_j$, their relative transformation $\mathbf{z}_{ij}$ is estimated via rigid pairwise registration using a mask for non-image areas, random pixel sampling, and Conjugate Gradient Line Search. As no significant differences were found across similarity metrics, mean square similarity was chosen for its efficiency. The information matrix $\mathbf{\Omega}_{ij}$ is chosen as the inverse of the covariance matrix of the positions and orientations, in combination with the inverse of the final mean squares similarity metric used for registration. In addition, the information matrix scales translation and orientation errors to the same order of magnitude.

The first node is fixed to prevent drift during optimization. Registration measurements are incorporated as sequential transformations ${}^{i-1}_{i}\mathbf{T}$, with additional non-adjacent transformations ${}^{i-1}_{i+1}\mathbf{T}$ for regularization. Loop closures, identified via EM tracking, reduce drift by linking nodes with overlapping features. Additional sparse EM-tracking measurements are included. Figure 1 illustrates the graph connections. Registrations identify clear features in overlapping US volumes while EM-tracking prevents drifting by providing global context.

2.4 Inter-Phase Edges

Inter-phase edges connect intra-phase graphs of neighboring phases through measurements of catheter motion, expressed as rigid transformations. Since image changes arise from catheter motion and cardiac deformation, these effects must be decoupled. Assuming minimal deformation, an affine transformation jointly optimizes catheter motion and deformation by registering US images from neighboring cardiac phases. A rigid transformation is then extracted to isolate catheter motion. The affine transformation consists of a linear transformation $\mathbf{A} \in \mathbf{R}^{3\times3}$

and a translation vector $\mathbf{t} \in \mathbf{R}^3$. The matrix $\mathbf{A}$ contains rotation, scaling, and shearing. By applying polar decomposition, $\mathbf{A}$ a can be represented as

$$\mathbf{A} = \mathbf{RS} \tag{4}$$

where $\mathbf{R}$ is orthogonal matrix representing the pure rotation, and $\mathbf{S}$ contains the scaling and shearing. Lastly, $\det(\mathbf{R}) = +1$ is verified to exclude reflections. This decomposition affects only the linear component $\mathbf{A}$ of the affine transformation, while the translation $\mathbf{t}$ remains unchanged.

Combining all measurements in a PGO maximizes the likelihood of observation by minimizing the error function of (1). This yields the optimal configuration of nodes $\mathbf{x}^*$, which hold the parameters for $\mathbf{T}_{\mathbf{p}_t,\mathbf{q}_t}$ to generate the dynamic panoramic reconstruction.

3 Experiments

The ICE data is acquired with a novel ICE system developed by LUMA Vision [5] that provides 3D US volumes in real-time. Fig. 1 shows the geometry of a US volume as a 2D plane in colored outlines, where the fan shape revolves around the center axis, resulting in a 360° FoV. The EM sensor is embedded near the US transducer with a known offset.

Our method is tested on a dynamic silicon phantom modeling the superior vena cava (SVC), inferior vena cava (IVC), and cardiac chambers. Static and dynamic acquisitions were performed on a static and pump-driven beating phantom, respectively, with the latter introducing substantial EM-field noise, representative of clinical conditions. The static and dynamic panoramic reconstruction used 60 and 230 US volumes, respectively. While our approach allows any number of cardiac phases, the dynamic sequence was discretized into five cardiac phases to capture the full motion range while limiting manual annotation. Although additional phases improve registration accuracy, they increase computational complexity. The ICE catheter follows a trajectory from the SVC to the IVC and back, challenging the method to handle revisited areas.

While a CT scan of the phantom is available, classifying its walls in US and CT data is error-prone due to their smooth, cornerless structure, making landmark annotation unreliable. With no alternative ground truth, we use a quantifiable setup with 3D-printed cones as landmarks, similar to [15], fixed beneath the phantom. Cone tips are annotated in US volumes, and annotations are transformed into the global frame for comparison with ground truth landmarks.

Reconstruction accuracy is evaluated using **feature error** and **global error**. Feature error quantifies the spread of multiple instances of a feature, indicating duplication or blurring, defined as the mean pairwise distance between predicted landmark labels. Global error measures alignment to ground truth as the mean Euclidean distance between true and predicted locations.

[5] LUMA Vision Ltd., Dublin, Ireland, www.lumavision.com

4 Results and Discussion

Quantative Results The results from the quantifiable setup, presented in Sect. 3, are shown in Fig. 2, where the distribution of annotations around their ground truth landmark is visualized for the baseline and our method, respectively. Table 1 presents results for different configurations in static and dynamic environments. Experiments 3–5 and 7–10 evaluate individual components of our proposed method, with Experiment 9 corresponding to the complete approach. Sequential registration significantly reduces feature error compared to raw and smoothed EM-tracking but introduces drift, increasing global error. Incorporating EM-tracking into the pose graph provides global information, reducing both errors compared to the baseline of EM-tracking, but slightly increasing feature error. Sparse EM-tracking preserves local accuracy while mitigating global drift.

In the dynamic case, intra-phase pose graphs without inter-graph edges reduce feature error compared to smoothed [6] EM-tracking but suffers from drift. Sparse EM-tracking mitigates drift, similar to the static case. Adding inter-graph edges regularizes drift between phase-neighboring graphs, further reducing feature error. A mean global error increase of 0.2 mm is negligible for navigation, while the focus remains on minimizing feature error to optimize image clarity. Despite pronounced EM-tracking noise, indicated by a 43% increase in feature error and a 22.4% increase in global error when comparing static and dynamic conditions, our method significantly enhances tracking accuracy. An ablation study tested the cyclic environment assumption, where sequential registration across cardiac phases with sparse EM-tracking results in an increased feature and global error, highlighting the role of intra- and inter-phase edges.

Qualitative Results ImFusion Suite [7] was used for visualization, blending voxel intensities using distance-to-border fusion. Panoramic reconstructions were

[6] Excessive noise makes raw EM-tracking unviable for the dynamic case.

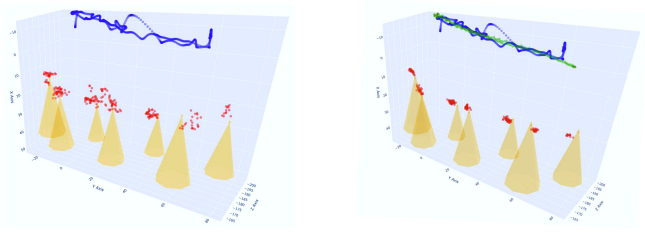

(a) **(b)**

Fig. 2. Experimental setup with cones as landmarks, smoothed EM-tracking trajectory (blue), and the reconstructed trajectory (green). Red points indicate projected annotations in the global frame based on the respective US volume pose. Annotation estimates from (a) EM-tracking and (b) our method are shown.

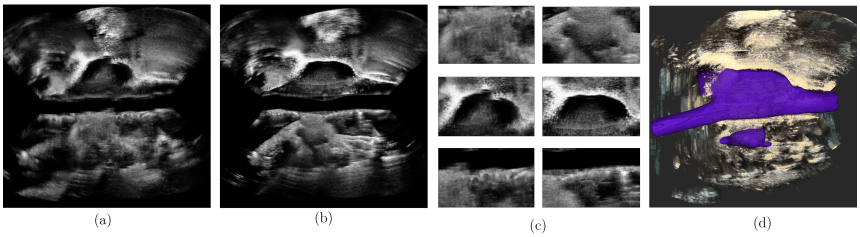

Fig. 3. Maps of the cardiac chambers of a silicon heart phantom using EM tracking (a) and our method (b) as a 2D plane from fused 3D reconstruction. Zoomed-in comparisons are shown in (c), with (d) providing a qualitative comparison to a CT scan.

generated based on EM tracking and the proposed method, differing only in volume poses, resulting in a dense 3D US volume with an extended FoV. Fig. 3 compares a 2D plane of volumetric reconstructions from a silicon heart phantom. The reconstruction based on EM-Tracking (a) shows discontinuities in the right atrium, SVC, and IVC and blurring of the right pulmonary veins. The reconstruction based on our proposed method (b) shows clear borders and visible right pulmonary veins. The shape of the right atrium changed, which was validated by aligning a CT scan of the silicon phantom with our reconstruction (d), showing good agreement of the IVC, SVC, and right atrium [7].

Runtime Using PGO with pairwise registration enables efficient handling of US volumes by decoupling global pose refinement from image content. Pairwise registrations, which are independent and parallelizable, take ∼3 seconds each

[7] The atrial appendage is missing in (a) and (b) due to the phantom's high reflectivity.

Table 1. Comparison of methods for reconstructing a static and dynamic silicon heart phantom, evaluated by feature and global error, with EM-tracking as a baseline.

Method	**Feature Error [mm]**	**Global Error [mm]**
Static Environment		
1) Raw EM Tracking	5.11 ± 3.82	5.79 ± 2.88
2) Smoothed EM Tracking	4.69 ± 3.92	5.48 ± 2.74
3) Sequential Registration	2.08 ± 1.42	8.58 ± 4.68
4) Intra-Phase Graph Dense EM Tracking	3.08 ± 2.86	4.65 ± 1.86
5) Intra-Phase Graph Sparse EM Tracking	1.81 ± 1.21	3.27 ± 1.04
Dynamic Environment		
6) Smoothed EM Tracking	6.74 ± 4.56	6.71 ± 3.66
7) Unconnected Intra-Phase Graphs	2.66 ± 1.55	7.96 ± 3.87
8) Unconnected Intra-Phase Graphs Sparse EM Tracking	2.57 ± 1.55	4.07 ± 1.86
9) **ICE-PoGO**	**2.47 ± 1.48**	**4.28 ± 1.75**
10) Affine Sequential Registration with EM Tracking	2.95 ± 2.00	4.33 ± 1.89

(Intel Core i7-10875H in Python) with geometric center initialization. The PGO step completes in under 1 second and can achieve real-time performance [9].

5 Conclusion

We demonstrated a method of dynamic panoramic reconstruction that addresses the challenges specific to 4D ICE through improved tracking of the imaging catheter. Introducing a hypergraph in PGO allows for joint optimization of poses across cardiac phases and increases temporal resolution in navigation and cardiac anatomy reconstruction. Efficient image use enables dynamic panoramic ICE reconstruction, addressing the demand for a large number of volumes. The approach was tested in a dynamic silicon phantom, showing both significant quantitative and qualitative improvements over the baseline of static panoramic reconstruction of gated volumes based on EM tracking. These improvements provide better anatomical context and guidance, increasing usability for clinicians and, we hope, will result in improved patient outcomes in the future.

Acknowledgments. This work was supported by the HINAV project funded by the Bavarian State Ministry for Economic Affairs, Regional Development and Energy.

Disclosure of Interests. The authors have no competing interests to declare that are relevant to the content of this article.

References

1. Brochet, E., Habib, G.: Intracardiac echocardiography during percutaneous closure of atrial septal defect and patent foramen ovale. Archives des maladies du coeur et des vaisseaux **98 Spec No 3**, 25–28 (2005)
2. Franz, A.M., Haidegger, T., Birkfellner, W., Cleary, K., Peters, T.M., Maier-Hein, L.: Electromagnetic tracking in medicine—a review of technology, validation, and applications. IEEE Transactions on Medical Imaging **33**(8), 1702–1725 (2014). https://doi.org/10.1109/TMI.2014.2321777
3. Freitas-Ferraz, A.B., Bernier, M., Vaillancourt, R., Ugalde, P.A., Nicodème, F., Paradis, J.M., Champagne, J., O'Hara, G., Junquera, L., del Val, D., Muntané-Carol, G., O'Connor, K., Beaudoin, J., Rodés-Cabau, J.: Safety of transesophageal echocardiography to guide structural cardiac interventions. Journal of the American College of Cardiology **75**(25), 3164–3173 (2020). https://doi.org/https://doi.org/10.1016/j.jacc.2020.04.069, https://www.sciencedirect.com/science/article/pii/S0735109720352268
4. Grisetti, G., Kümmerle, R., Stachniss, C., Burgard, W.: A tutorial on graph-based slam. IEEE Intelligent Transportation Systems Magazine **2**(4), 31–43 (2010). https://doi.org/10.1109/MITS.2010.939925
5. Hickler, J., Neary-Zajiczek, L., Bandaru, R.S., Balle Sánchez, M., Hennersperger, C., Wörz, S.: Panoramic anatomical context in 3d intracardiac echocardiography (ice) with 3d registration and geometry-based image fusion. In: Camara, O., Puyol-Antón, E., Sermesant, M., Suinesiaputra, A., Zhao, J., Wang, C., Tao, Q., Young, A. (eds.) Statistical Atlases and Computational Models of the Heart. Workshop,

CMRxRecon and MBAS Challenge Papers. pp. 87–97. Springer Nature Switzerland, Cham (2025)
6. Hu, T., Chen, T., Maduray, K., Han, W., Zhong, J.: Intracardiac echocardiography: An invaluable tool in electrophysiological interventions for atrial fibrillation and supraventricular tachycardia. Reviews in Cardiovascular Medicine **25**(6), 191 (Jun 2024). https://doi.org/10.31083/j.rcm2506191, https://doi.org/10.31083/j.rcm2506191, published by IMR Press
7. ImFusion GmbH: ImFusion Suite for Academia, Version 2.47.0 [Software]. ImFusion GmbH, Munich, Germany (2023), available from: https://www.imfusion.com
8. Koolwal, A.B., Barbagli, F., Carlson, C.R., Liang, D.H.: A fast slam approach to freehand 3-d ultrasound reconstruction for catheter ablation guidance in the left atrium. Ultrasound in medicine & biology **37 12**, 2037–54 (2011), https://api.semanticscholar.org/CorpusID:23245728
9. Kümmerle, R., Grisetti, G., Strasdat, H., Konolige, K., Burgard, W.: G2o: A general framework for graph optimization. In: 2011 IEEE International Conference on Robotics and Automation. pp. 3607–3613 (2011). https://doi.org/10.1109/ICRA.2011.5979949
10. Mao, Z.: Three-dimensional Ultrasound Fusion for Transesophageal Echocardiography. Phd thesis, University of Technology Sydney (UTS) (2023), http://hdl.handle.net/10453/173499
11. Mao, Z., Zhao, L., Huang, S., Fan, Y., Lee, A.P.W.: Dsr: Direct simultaneous registration for multiple 3d images. In: Wang, L., Dou, Q., Fletcher, P.T., Speidel, S., Li, S. (eds.) Medical Image Computing and Computer Assisted Intervention – MICCAI 2022. pp. 98–107. Springer Nature Switzerland, Cham (2022)
12. OpenStax College: Anatomy & physiology, connexions web site (6 2013), http://cnx.org/content/col11496/1.6/
13. Pham, T.H., Singh, G.D.: 3d intracardiac echocardiography for structural heart interventions. Interventional Cardiology Clinics **13**(1), 11–17 (2024). https://doi.org/https://doi.org/10.1016/j.iccl.2023.08.005, https://www.sciencedirect.com/science/article/pii/S2211745823000676, multi-Modality Interventional Imaging
14. Rigatelli, G., Cardaioli, P., Giordan, M., Dell'Avvocata, F., Braggion, G., Piergentili, C., Roncon, L., Faggian, G.: Transcatheter intracardiac echocardiography-assisted closure of interatrial shunts: complications and midterm follow-up. Echocardiography **26**(2), 196–202 (2 2009). https://doi.org/10.1111/j.1540-8175.2008.00763.x
15. Ronchetti, M., Rackerseder, J., Tirindelli, M., Salehi, M., Navab, N., Wein, W., Zettinig, O.: Pro-tip: Phantom for robust automatic ultrasound calibration by tip detection. In: Wang, L., Dou, Q., Fletcher, P.T., Speidel, S., Li, S. (eds.) Medical Image Computing and Computer Assisted Intervention – MICCAI 2022. pp. 84–93. Springer Nature Switzerland, Cham (2022)
16. Tang, G.H., Zaid, S., Hahn, R.T., Aggarwal, V., Alkhouli, M., Aman, E., Berti, S., Chandrashekhar, Y., Chadderdon, S.M., D'Agostino, A., Fam, N.P., Ho, E.C., Kliger, C., Kodali, S.K., Krishnamoorthy, P., Latib, A., Lerakis, S., Lim, D.S., Mahadevan, V.S., Nair, D.G., Narula, J., O'Gara, P.T., Packer, D.L., Praz, F., Rogers, J.H., Ruf, T.F., Sanchez, C.E., Sharma, A., Singh, G.D., van Mieghem, N.M., Vannan, M.A., Yadav, P.K., Ya'Qoub, L., Zahr, F.E., von Bardeleben, R.S.: Structural heart imaging using 3-dimensional intracardiac echocardiography: Jacc: Cardiovascular imaging position statement. JACC: Cardiovascular Imaging **18**(1), 93–115 (2025). https://doi.org/https://doi.org/10.1016/j.jcmg.2024.05.012, https://www.sciencedirect.com/science/article/pii/S1936878X2400202X

17. Wachinger, C., Navab, N.: Simultaneous registration of multiple images: Similarity metrics and efficient optimization. IEEE Transactions on Pattern Analysis and Machine Intelligence **35**(5), 1221–1233 (2013). https://doi.org/10.1109/TPAMI.2012.196
18. Wachinger, C., Wein, W., Navab, N.: Three-dimensional ultrasound mosaicing. In: Ayache, N., Ourselin, S., Maeder, A. (eds.) Medical Image Computing and Computer-Assisted Intervention – MICCAI 2007. pp. 327–335. Springer Berlin Heidelberg, Berlin, Heidelberg (2007)
19. Zhang, L., Wahle, A., Chen, Z., Zhang, L., Downe, R.W., Kovarnik, T., Sonka, M.: Simultaneous registration of location and orientation in intravascular ultrasound pullbacks pairs via 3d graph-based optimization. IEEE Transactions on Medical Imaging **34**(12), 2550–2561 (2015). https://doi.org/10.1109/TMI.2015.2444815